Magnesium Technology 2012
Edited by: Suveen N. Mathaudhu, Wim H. Sillekens, Neale R. Neelameggham, and Norbert Hort
TMS (The Minerals, Metals & Materials Society), 2012

MICROSTRUCTURE AND MECHANICAL PROPERTIES OF HIGH PRESSURE DIE CAST AM50 MAGNESIUM ALLOY CONTAINING Ce

Faruk Mert[1,2], Ahmet Özdemir[1], Karl Ulrich Kainer[2] and Norbert Hort[2]
[1] Gazi University, Faculty of Technology, Department of Manufacturing Engineering, TR-06500 Ankara - TURKEY
[2] Helmholtz-Zentrum Geesthacht, Magnesium Innovation Centre, Max-Planck-Straße 1, D-21502 Geesthacht - GERMANY

Keywords: Microstructure, Mechanical properties, AM50, Cerium, High pressure die casting

Abstract

Over the past decades, the necessity to decrease the weight of automobile parts has created a considerable interest in magnesium alloys. The need to develop magnesium die casting alloys for car components motivates R&D in high temperature magnesium alloy development. In order to improve magnesium alloys with low cost, high strength and with notable elevated temperature properties, the effect of Ce addition (0.5/1.0 wt.-%) on microstructure and mechanical properties of AM50 was studied. Results show that addition of Ce to AM50 resulted in grain refinement and the formation of the secondary phase $Al_{11}Ce_3$. Mechanical properties of investigated alloys at both room and elevated temperature were remarkably increased. AM50 containing 1%wt. Ce showed relatively better refinement and mechanical properties compared to AM50 with 0.5%wt. Ce.

Introduction

Weight reduction in automotive industry is very attractive in recent years due to potential of fuel efficiencies and lower CO_2 emission levels. Magnesium alloys are one of the lightest in engineering materials. High Pressure Die Casting (HPDC) is the most preferred process to produce magnesium parts for automotive as well as for numerous other applications [1, 2]. Some widely used commercial magnesium alloys, such as AZ91, AM50 and AM60, have already been applied to automobile components, such as seat frames, steering wheels, instrument panels, brackets, fans, etc [3]. However, some commercial application of magnesium alloys for important structural components is limited due to poor mechanical properties at elevated temperatures [4-6].

Nonetheless, the demand of magnesium applications in automotive parts has been increasing, so that new magnesium alloys having low cost and high elevated temperature properties are needed to develop. Hence, more studies have been devoted to develop new magnesium alloys mainly based on Mg-Al-RE (RE = rare earth), Mg-Al-Ca/Sr and Mg-Al-Si systems, which have improved elevated temperature performance [7-13]. Among them, Mg-Al-RE system show a significant improvement in heat-resistant Mg-Al based alloys due to formation of thermal stable $Al_{11}RE_3$ precipitates and complete suppression of the $Mg_{17}Al_{12}$ phase [14, 15]. Even though the influences some RE, such as La, Pr and Nd, on the microstructure and mechanical properties of HPDC AM40 alloy was investigated [7-9], studies on effects of single Ce element addition on microstructure and mechanical properties of HPDC AM50 alloy is quite limited. Thus, this study investigates the influence of different amounts of Ce on phase formation and microstructure development as well as its influences on mechanical properties at different temperatures in order to contribute for the development of new Mg-RE alloys.

Experimental Procedure

Cerium additions of 0.5 wt.% and 1.0 wt.% were made to the base AM50 alloy. Three compositions are referred as AM50, AM50Ce0.5 and AM50Ce1, respectively. The alloys were cast into step-shape plate with four different step thicknesses (2, 6, 10, 14 mm) as seen in Fig. 1. 14 mm section was used for the present studies.

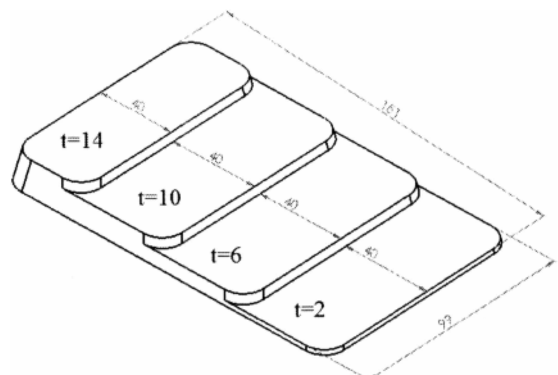

Fig. 1. HPDC step plates with different thickness.

A Frech DAK-450 cold chamber die casting machine was used for casting experiments and 30 shots have been made for each alloy. Die casting conditions and parameters are demonstrated in Table 1.

Table 1. Experimental die casting conditions

Parameter	Value
Melt temperature	680 °C
Casting pressure	40 MPa
Die temperature	200 °C
Shot sleeve speed	5 m/s
Protective gas	Mixture of N_2 and 2 vol.% SF_6
Machine	Frech DAK 450 (cold chamber)

Samples (20x10x10 mm) were taken from 14 mm section of the step plates for microstructural observation and hardness tests. These samples were ground with 800, 1200, 2400 grit silicon carbide emery papers. After last grinding step, the specimens were washed with water, rinsed with ethanol and dried. The final polishing was conducted with OPS™ suspension (Struers). The chemical compositions of the alloys were analyzed using a Spark Emission Analyser, Spectrolab9 from SPECTRO (Kleve, Germany). The specimens were chemically etched using a combination of acetic acid, picric acid, ethanol, and purified water to reveal the microstructure. Microstructure was investigated by

Leica DMI 5000 optical microscopy and Zeiss Ultra55 scanning electron microscopy (SEM) equipped with energy dispersive X-ray analysis (EDX). Grain sizes were determined using the line intercept method [16]. The XRD measurements were performed on a Siemens D5000 machine using Cu-Kα_1 radiation (wavelength λ=0.15406 nm). The diffraction patterns were measured from 2Θ (15-75°) for each sample. The increment was 0.04° and the step time was 6.4 s. The hardness tests were carried out by Vickers hardness on Emcotest M1C010 automated hardness test machine; the test load, the dwell time and the repetition were 5 kg, 10 s and 10 times. Tension and compression tests were performed at room temperature and elevated temperatures (100 °C, 120 °C, 150 °C) using a Zwick 050 testing machine according to DIN EN 10002 [17] and DIN 50106 [18]. Specimens used in tension tests with a gauge length of 30 mm, a diameter of 6 mm and threaded heads were machined according to ASTM E8M-09 [19]. The compression specimens were cylinders with a height of 16.5 mm and a diameter of 11 mm. Both tension and compression tests were done under a strain rate of 1×10^{-3} s^{-1}. In order to obtain homogenous temperature, the samples were soaked at the test temperatures (except RT) for 10 minutes before test run. All tests were repeated at least three times.

Results and Discussion

Microstructures

The chemical composition of investigated die casting magnesium alloys was analyzed and given in Table 2.

Table 2. Chemical composition of investigated alloys (wt.%).

Alloy	Mg	Al	Mn	Ce
AM50	Bal.	4,78	0,43	-
AM50Ce0.5	Bal.	4,67	0,35	0,53
AM50Ce1	Bal.	4,49	0,32	1,02

The X-ray diffraction (XRD) patterns of investigated alloys are demonstrated in Fig. 2. AM50 alloy is mostly consisted of Mg and $Mg_{17}Al_{12}$ phases [20]. It can be seen in Fig 2, two different phases are detected in the microstructure of AM50 alloy, whereas three different phases are detected in the microstructure of AM50Ce0.5 and AM50Ce1 alloy as a result of Ce addition. When Ce added to AM50 alloy, the diffraction peaks of $Mg_{17}Al_{12}$ phase decrease and go down the detection limit of XRD machine. The main secondary phase in the AM50Ce0.5 and AM50Ce1 alloys is $Al_{11}Ce_3$.

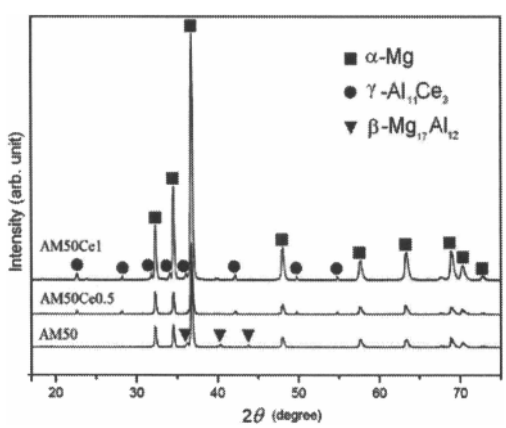

Fig. 2. XRD patterns of investigated alloys

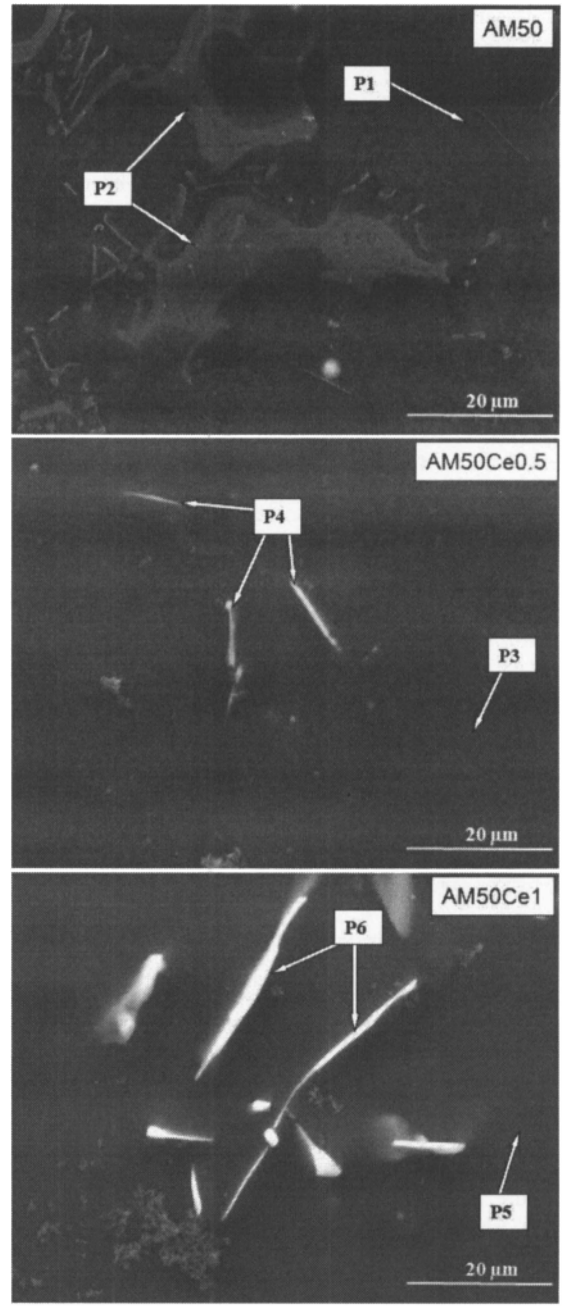

Fig. 3. SEM images of investigated alloys

Fig. 3 shows SEM morphology of investigated alloys. α-Mg and intermetallic constituents appeared in AM50 alloy. EDX study was done on selected points as shown in AM50. The results show that P1 is on α-Mg matrix, P2 is on β-$Mg_{17}Al_{12}$ intermetallic compound. When 0.5wt.% Ce was added to AM50 alloy, as seen in AM50Ce0.5, new γ-$Al_{11}Ce_3$ phase occurred and it appeared as needle-shaped. As Ce amount was increased from 0.5% to 1%, also γ-$Al_{11}Ce_3$ phase amount clearly increased in AM50Ce1 alloy. Similar EDX study was done again in AM50Ce1 and EDX results show that P5 is on α-Mg, and P6 is on γ-$Al_{11}Ce_3$ in AM50Ce1 alloy. Similar situation can be seen in AM50Ce0.5 alloy, but γ-$Al_{11}Ce_3$ phase was less comparing to AM50Ce1 alloy because of Ce amount. As shown in Fig. 3, Ce addition decreases the fraction of β-$Mg_{17}Al_{12}$ phase and facilitates to form γ-$Al_{11}Ce_3$. The overall EDX results of AM50 and with 0.5 and 1wt.% content of Ce are shown Table 3. According to these results, it can be easily said that addition of Ce causes the formation of new γ-$Al_{11}Ce_3$ phase.

Table 3. EDX result of constituent phases of investigated alloys from Fig. 3 (at.%)

Location	n_{Mg}/n_{Al}	n_{Al}/n_{Ce}
P1	96.54/3.12	---
P2	62.33/27.16	---
P3	96.67/2.98	---
P4	---	45.18/15.02
P5	98.09/1.76	---
P6	---	53.34/17.11

Fig. 4 demonstrates microstructure of studied alloys. It can be seen that the microstructure of AM50 alloy mainly comprises of α-Mg and β-$Mg_{17}Al_{12}$ phases. $Mg_{17}Al_{12}$ phase formed along grain boundaries as network. When Ce is added to AM50, a new phase occurs. Since solid solubility of Ce in Mg-matrix solid solution of AM50 magnesium alloy is low, this phase contains mostly Al and Ce [21]. The Al-Ce phase often appears in between the $Mg_{17}Al_{12}$ phase, possibly providing obstructions to the growth of $Mg_{17}Al_{12}$, breaking up its networked structure. Hence, Ce addition is proved to be beneficial to refining the grain size of AM50 alloy [22]. The grain size decreases with the addition of Ce from 0.5wt.% to 1wt.%, as shown in Table 4.

Table 4. Grain size of investigated alloys.

Alloy	Grain size [μm]
AM50	42 (±7)
AM50Ce0.5	33 (±6)
AM50Ce1	24 (±4)

Mechanical properties

The relationship between hardness and Ce addition is demonstrated in Table 5. Hardness of investigated alloys increases clearly with increasing amounts of Ce.

Table 5. Hardness result of the investigated alloys.

Alloy	Hardness [HV]
AM50	38 (±6)
AM50Ce0.5	40 (±9)
AM50Ce1	45 (±7)

Fig. 5 shows tensile properties of the investigated alloys tested at room and elevated temperatures. The alloys show the highest tensile yield strength (TYS) and ultimate tensile strength (UTS) at room temperature (RT). Typically, the TYS and UTS decrease, while elongation increases with the increase of the temperature. It can be seen that the addition of Ce can remarkably improve the tensile properties of AM50 alloys at different temperatures.

From Fig. 5a, it is obvious that AM50 shows the lowest TYS, while with addition of Ce, the TYS is remarkably improved both at room and elevated temperatures. The TYS of AM50 is 87 MPa at RT and 69 MPa at 150 °C, whereas for AM50Ce1 the TYS is 98 MPa at RT and 80 MPa at 150 °C.

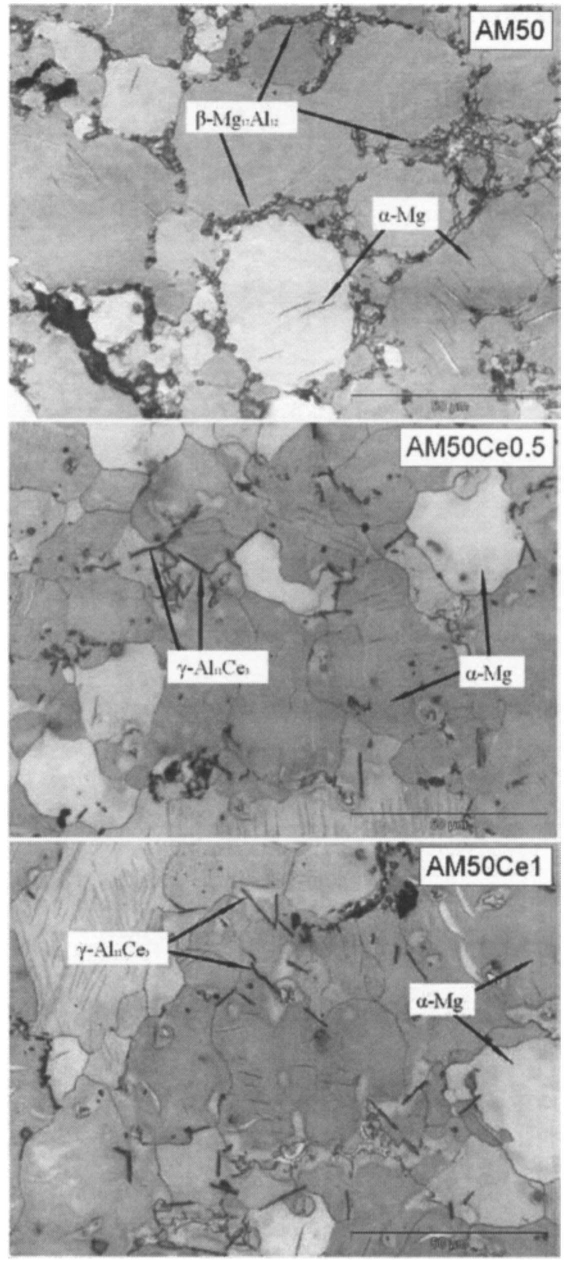

Fig. 4. Microstructures of investigated alloys

The UTS has same trend as TYS with the change of Ce content (Fig. 5b). The UTS of AM50 is 145 MPa at RT and 120 MPa at 150 °C, while for AM50Ce1 the UTS is 168 MPa at RT and 137 MPa at 150 °C. The elongation of the alloys is also improved as the result of Ce addition and at all temperatures the highest value is acquired from AM50Ce1 (Fig. 5c). For example, the elongation of AM50 are 2,80% at RT and 8,31% at 150 °C, whereas for AMCe1 the elongation are 4,82% at RT and 10,30% at 150 °C. The elongation of the investigated alloys increases with the increase of the temperature and reaches a highest value at 150 °C.

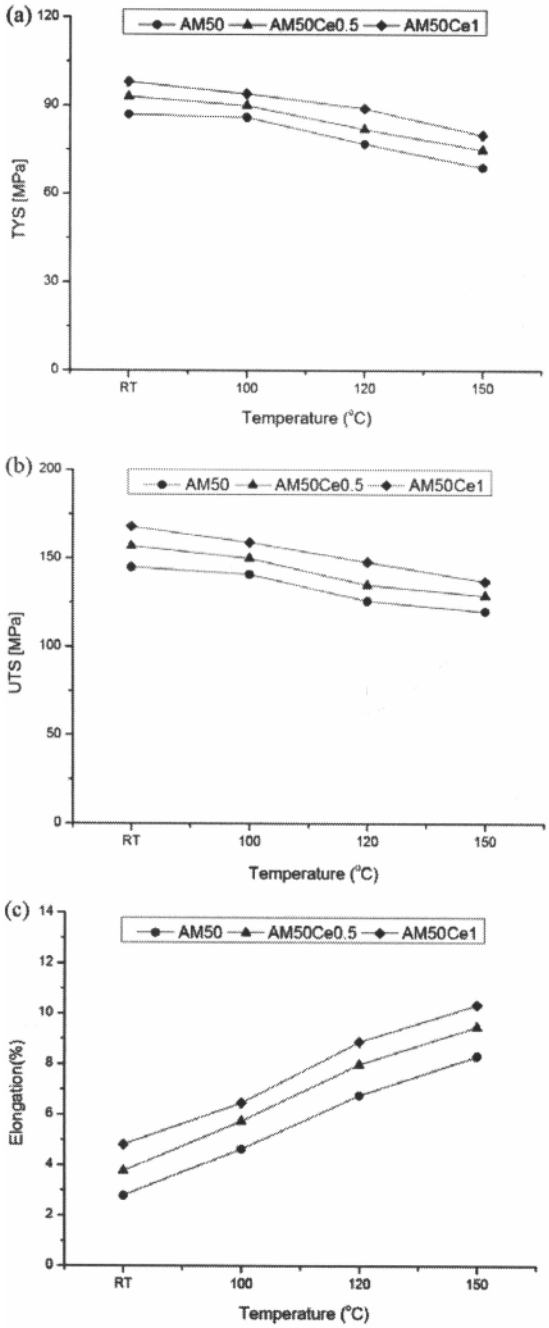

Fig. 5. Tensile properties of investigated alloys at different temperatures: a)TYS, b)UTS, c)Elongation.

In previous studies, the effect of RE on the microstructure and mechanical properties of AM series magnesium alloy has been investigated [8, 9, 21-23]. These studies indicate that four RE elements (La, Ce, Pr, Nd) can improve the mechanical properties of AM series magnesium alloys and strengthening effect increases with increasing RE content. The present work is good agreement with previous studies.

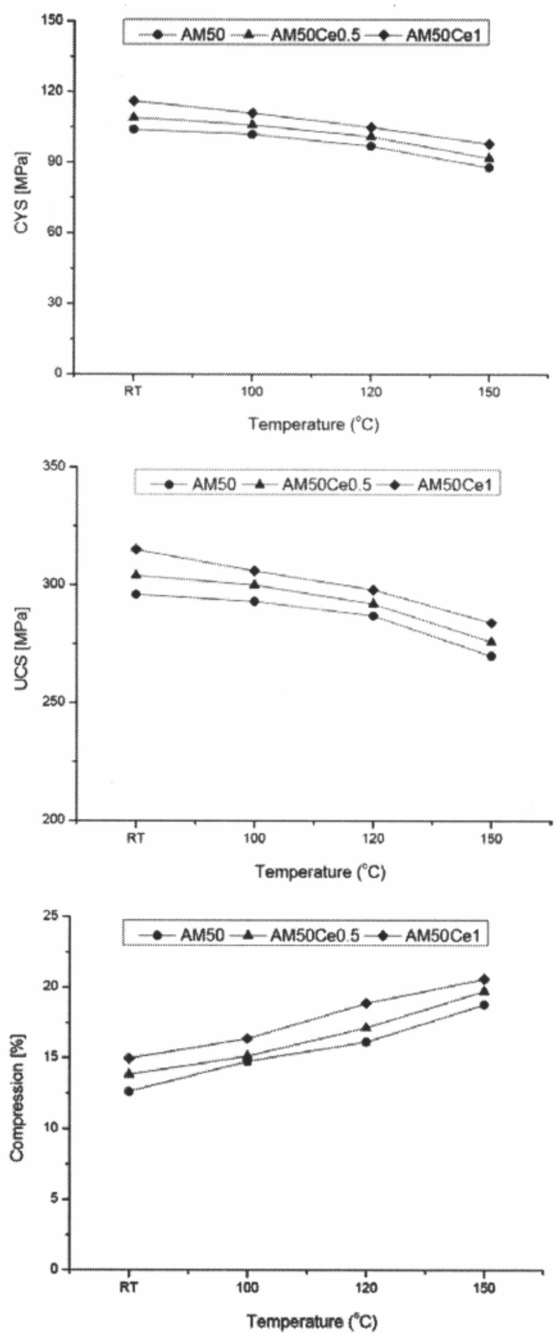

Fig. 6. Compressive properties of investigated alloys at different temperatures: a)CYS, b)UCS, c)Compression.

Compressive yield strength (CYS) and ultimate compressive strength (UCS) have same trends both at room and elevated temperature as TYS and UTS at different temperatures. From Fig. 6a, it is obvious that AM50 exhibits the lowest CYS, while with addition of Ce, the CYS is remarkably improved both at room and elevated temperatures. The CYS of AM50 is 104 MPa at RT and 88 MPa at 150 °C, whereas for AM50Ce1 the CYS are 116 MPa at RT and 98 MPa at 150 °C. The UCS of the alloys has the general same changing rules with CYS after addition of Ce (Fig. 6b). The UCS of AM50 alloy are 296 MPa at RT and 270 MPa at 150 °C, while for AM50Ce1 alloy the UCS are 315 MPa at RT and 284 MPa at 150 °C, respectively. The compression of the alloys is also developed as the result of Ce addition and at all temperatures; the highest value is obtained from AMCe1 alloy (Fig. 6c). For example, the compression of AM50 are 12,6% at RT and 18,78% at 150 °C, whereas for AMCe1 the compression are 14,96% at RT and 20,6% at 150 °C, respectively. The deformation in compression of the alloys investigated increases with the increase of the temperature and reaches a highest value at 150 °C.

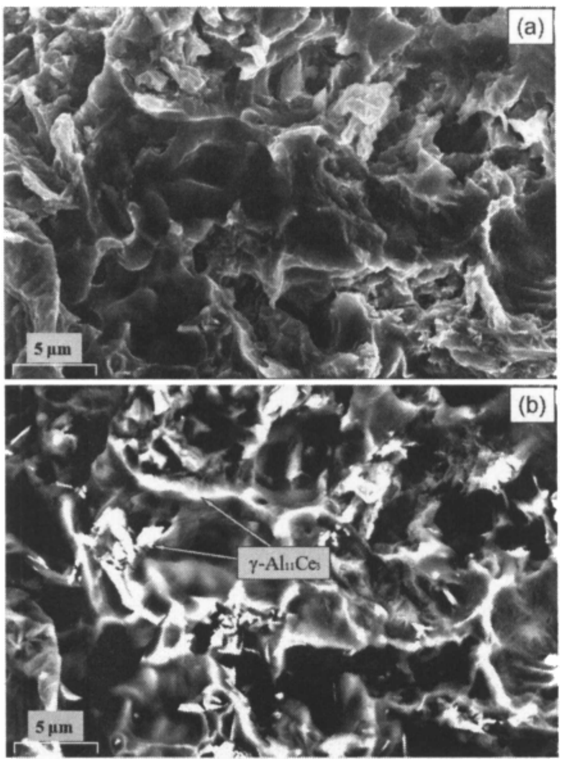

Fig. 7. SEM observation of the fracture surface of AM50Ce1 alloy at RT: (a) secondary electron image, and (b) backscattered electron image.

Backscatter SEM fracture images of HPDC AM50Ce1 alloy at RT are shown in Fig. 7. The failure surface of AM50Ce1 alloy is composed of tearing ridge and cleavage-type facets. Also, large numbers of ductile dimples can be observed obviously. It shows the mixed characteristics of fracture. There are more ductile dimples and characters of quasi-cleavage on the fracture surface of AM50Ce1 alloy (Fig. 7b). Significantly, almost all the $Al_{11}Ce_3$ precipitates are distributed around the dimples. This indicates that before fracture the alloy has undergone certain plastic deformation, and the fine $Al_{11}Ce_3$ particles are not the main crack sources.

With addition of Ce, the grains of α-Mg matrix are refined and eutectic phase β-$Mg_{17}Al_{12}$ is suppressed and substituted by $Al_{11}Ce_3$ with the former being the dominant one. Because obtaining of $Al_{11}Ce_3$ particles when Ce was added to AM50 could refine the grain size significantly. Small grain size can effectively prevent the dislocation slip, so that deformation of fine grain structural alloys needs higher stress. The main strengthening phase in AM50 alloy is β-$Mg_{17}Al_{12}$, which has low melting point (with eutectic temperature of 437 °C) and a poor thermal stability. β-$Mg_{17}Al_{12}$ phase can readily soften and coarsen at the temperature exceeding 125 °C [24]. Addition of Ce to AM50 results in the suppression of β-$Mg_{17}Al_{12}$ phase and the formation of $Al_{11}Ce_3$ phase. $Al_{11}Ce_3$ phase has a high melting point (>1200°C), and then the softening temperature of the alloy containing $Al_{11}Ce_3$ phase can be increased. With the increase of Ce content in the alloys, the amount of $Al_{11}Ce_3$ particles increases significantly, and then the strengthening effect is also improved. Thermally stable $Al_{11}Ce_3$ phase was formed after addition of Ce, which is located at grain boundaries and suppressed the slippage of grain boundary at elevated temperature, so that elevated temperature properties of the alloys are improved.

Summary

The microstructure and mechanical properties of HPDC AM50 alloys with Ce (0,5% and 1%) have been investigated. The main conclusions could be drawn as follows:

(1) Addition of Ce reduces grain size of AM50 alloy.

(2) The addition of Ce can remarkably improve tensile and compressive properties of AM50 alloys at room and elevated temperatures. This is due to Al-Ce phases on the one hand and grain refinement on the other hand.

Acknowledgements

The authors want to express their gratitude to G. Wiese, J. Bohlen, G. Meister, W. Punessen and S. Schubert for their technical support. Financial support from Turkey Council of Higher Education (YÖK) scholarship for Faruk's PhD study in Helmholtz-Zentrum Geesthacht is also appreciated.

References

[1] Külekçi, M.K., "Magnesium and its alloys applications in automotive industry," *International Journal of Advanced Manufacturing Technology*, 39 (2008), 851-865.

[2] Mordike, B.L. and Ebert, T., "Magnesium - Properties - applications – potential," *Materials Science and Engineering A*, 302 (2001), 37-45.

[3] Easton, M., Beer, A., Barnett, M., Davies, C., Dunlop, G., Durandet, Y., Blacket, S., Hilditch, T. Beggs, P., "Magnesium alloy applications in automotive structures," *Journal of the Minerals, Metals and Materials Society*, 60 (2008), 57-62.

[4] Luo A.A., "Recent magnesium alloy development for elevated temperatures applications," *International Material Reviews*, 49 (2004), 13-30.

[5] Powell, B.R., Ouiment, J.L., Allison, J.E., Haynes, J.A., Beals, R.S., Kopka, L., Reid, P.P., "The Magnesium Powertrain Cast Components Project: Part I – Accomplishments of Phase I and the Objectives and Plans for the Magnesium Engine in Phase II," in *Magnesium Technology 2004*, ed. Alan A. Luo, 2004, The Metals, Minerals and Materials Society, Charlotte, North Carolina, p.3-10.

[6] Bronfin, B., Aghion, E., Buch, F., Schumann, S., Katsir, M., "Die casting magnesium alloys for elevated temperatures applications," in *Magnesium Technology 2001*, ed. John N. Hryn,

The Metals, Minerals and Materials Society, 2001, New Orleans. Louisiana, p.127-130.
[7] Zhang, J., Zhang, M., Meng, J., Wu, R., Tang, D., "Microstructures and mechanical properties of heat-resistant high-pressure die-cast Mg-4A1-xLa-0.3Mn (x=1, 2, 4, 6) alloys," *Materials Science and Engineering A*, 527 (2010), 2527-2537.
[8] Zhang, J., Liu, K., Fang, D., Qiu, X., Yu, P., Tang, D., Meng, J., "Microstructures, mechanical properties and corrosion behavior of high-pressure die-cast Mg-4Al-0.4Mn-xPr (x=1, 2, 4, 6) alloys," *Journal of Alloys and Compounds*, 480 (2009), 810-819.
[9] Zhang, J., Wang, J., Qiu, X., Zhang, D., Tian, Z., Niu, X., Tang, D., Meng, J., "Effect of Nd on the microstructure, mechanical properties and corrosion behavior of die-cast Mg-4Al-based alloy," *Journal of Alloys and Compounds*, 464 (2008), 556-564.
[10] Kondori, B., Mahmudi, R., "Effect of Ca additions on the microstructure, thermal stability and mechanical properties of a cast AM60 magnesium alloy," *Materials Science And Engineering A*, 527 (2010), 2014-2021.
[11] TerBush, J.R., Suzuki, A., Saddock, N.D., Jones, J.W., Pollock, T.M., "Dislocation substructures of three die-cast Mg-Al-Ca-based alloys," *Scripta Materialia*, 58 (2008), 914-917.
[12] Czerwinski, F., Zielinska-Lipiec, A., "The microstructure evolution during semisolid molding of a creep-resistant Mg-5Al-2Sr alloy," *Acta Materialia*, 53(2005), 3433-3444.
[13] Srinivasan, A., Swaminathan, J., Pillai, U.T.S., Guguloth, K., Pai, B.C., "Effect of combined addition of Si and Sb on the microstructure and creep properties of AZ91 magnesium alloy," *Materials Science and Engineering A*, 485 (2008), 86-91.
[14] Bakke, P., Westengen, H., "Die casting for high performance-Focus on alloy development," *Advanced Engineering Materials*, 5 (2003), 879-885.
[15] Pettersen, G., Westengen, H., Hoier, R., Lohne, O., "Microstructure of a pressure die cast magnesium-4wt.% aluminium alloy modified with rare earth additions," *Materials Science and Engineering A*, 207 (1996), 115-120.
[16] ASTM E112-10 Standard test methods for determining average grain size, 2004.
[17] DIN EN ISO 10002, Tension Testing of Metallic Materials, Beuth Verlag, Berlin, 2001.
[18] DIN 50106, Compression Testing of Metallic Materials, Beuth Verlag, Berlin, Germany, 1978.
[19] ASTM E8M - 09 Standard Test Methods for Tension Testing of Metallic Materials, 2009.
[20] Materials Science International Team (MSIT), and Gröbner, J., Ran, Q., *Light Metal Ternary Systems: Phase Diagrams, Crystallographic and Thermodynamic Data*, Vol. 11A3, Part 3, Ed: Effenberg, G., Ilyenko, S., 2005, Springer Press, Berlin.
[21] Liao, H.M., Long, S.Y., Guo, C.B., Zhu, Z.B., "Effect of Ce-rich misch metal addition on sequeeze cast microstructure and mechanical properties of AZ81 alloy," *Transactions of Nonferrous Metals Society of China*, 18 (2008), 44-49.
[22] Liu, S.F., Huang, S.Y., Xu, P., "Influence of cerium addition on as-cast microstructure of AZ91 magnesium alloy," *Acta Metallurgica Sinica*, 42 (2006), 443-448.
23] Wang, M., Zhou, H., Wang, L., "Effect of yttrium and cerium addition on microstructure and mechanical properties of AM50 magnesium alloy," *Journal of Rare Earths*, 25 (2007), 233-237.
[24] Lü, Y., Wang, Q., Zeng, X., Ding, W., Zhai, C., Zhu, Y., "Effects of rare earths on the microstructure, properties and fracture behavior of Mg–Al alloys," *Materials Science and Engineering A*, 278 (1999), 66-76.